EDMS No. 359787

ORGANISATION EUROPEENNE POUR LA RECHERCHE NUCLEAIRE
EUROPEAN ORGANIZATION FOR NUCLEAR RESEARCH

Laboratoire Européen pour la Physique des Particules
European Laboratory for Particle Physics

Technical Inspection and Safety Division

Technical Note
CERN-TIS-2002-033-RP-**TN**

Beam and reference field monitoring during the 2002 CERF runs

E. Dimovasili and M. Silari

CERN, 1211 Geneva 23, Switzerland

Abstract

This note discusses beam and reference field monitoring at the CERF facility during the two runs in 2002. Two new instruments were installed in the irradiation cave. The first is a Multi-Wire Proportional Chamber for accurate measurements of the profile of the 120 GeV/c hadron beam impinging on the copper target. The second is an ionisation chamber of similar design as the reference CERF beam monitor (the PIC), put in place as a back-up instrument of the PIC. This chamber was first submitted to extensive performance tests with ^{137}Cs sources in the TIS/RP calibration laboratory and later tested and inter-compared with the PIC in the CERF hadron beam. In addition to the above developments, a complete mapping of the neutron field in the various reference exposure locations on the concrete top, iron top and concrete side were also performed with a Tissue Equivalent Proportional Counter (the HANDI TEPC) and the LINUS rem counter. The results agree well with measurements performed in previous years.

CERN, 1211 Geneva 23, Switzerland
1 October 2002

1. Introduction

This report discusses the results of various types of measurements carried out at the CERF (the CERN-EU high-energy Reference Field) [1] facility during the two runs in 2002 (13-19 June and 10-17 July). Before the start of the June run, two new instruments were installed in the beam line in the CERF irradiation cave. The first is a Multi-Wire Proportional Chamber (MWPC) for measurements of the beam profile; the second is a 5-litre volume ion chamber of the same design as the standard CERF beam monitor (the Precision Ionisation Chamber, PIC), called here BIG PIC. This note first discusses measurements of beam profile carried out with the MWPC. Next it describes performance tests of the BIG PIC with ^{137}Cs sources in the TIS/RP calibration laboratory and in-beam at CERF, and its inter-comparison with the standard PIC beam monitor. The results of the verification of the calibration factor of the standard PIC by inter-comparison with one of the scintillators of the H6 beam line (the Trigger 4), now routinely performed before each CERF run, are discussed elsewhere [2]. In addition to the above developments, the usual measurements at the various reference exposure locations were performed with the HANDI TEPC and the LINUS rem counter of the CERN Radiation Protection group. This notes provides the results of complete mapping of the neutron field on the concrete top, iron top and concrete side.

2. Measurements of beam profile by a Multi-Wire Proportional Chamber

Until last year a check of the beam shape and position at the CERF copper target was performed by taking images of the beam, originally with a radiographic film (see for example, ref. [3]) and since 1999 with a Polaroid film (which has the advantage of immediate development). X-ray films required development in the laboratory of the individual dosimetry service, so that the results were often available only after the run. This method was time consuming and only provided rough information on the "beam spot". The use of X-ray films allowed a reconstruction of the beam profile, but only by an off-line analysis [4].

The above method was good enough for the purpose of checking the correct alignment of the beam in the H6 line, which usually did not present any problem as the beam set-up was done by the operator from the Experimental Areas control room. However, doubts about the correct set-up of the beam in the October 2001 run suggested to look for a more reliable solution for checking the beam position and profile. Such solution was identified in a MWPC, which is one of the standard monitors used to measure the beam profile in the SPS secondary beam lines.

The MWPC was installed in-between the two CERF target positions, approximately one metre upstream of the one below the concrete roof-shield. As its effect on the beam is negligible, and because a retractable system is far more expensive than a fixed one, the MWPC was mounted on a static support so that it stays in the beam all the time. To measure the beam profile, the CERF copper target must obviously be removed from the upstream support (the one under the iron roof-shield). It was verified (by tests during the beam set-up) that backscattering from the target installed under the concrete roof-shield does not affect the profile measurement, so that in this case one can measure the beam profile on-line while taking data. An

example of the horizontal and vertical beam profiles measured with the MWPC is shown in Figure 1. Changing collimators C3 and C5 from ± 11 mm to ± 14 mm modifies the rms width of the beam in the two transverse dimensions from 10.4 mm (horizontally) and 9.1 mm (vertically) to 11.5 mm (horizontally) and 9 mm (vertically).

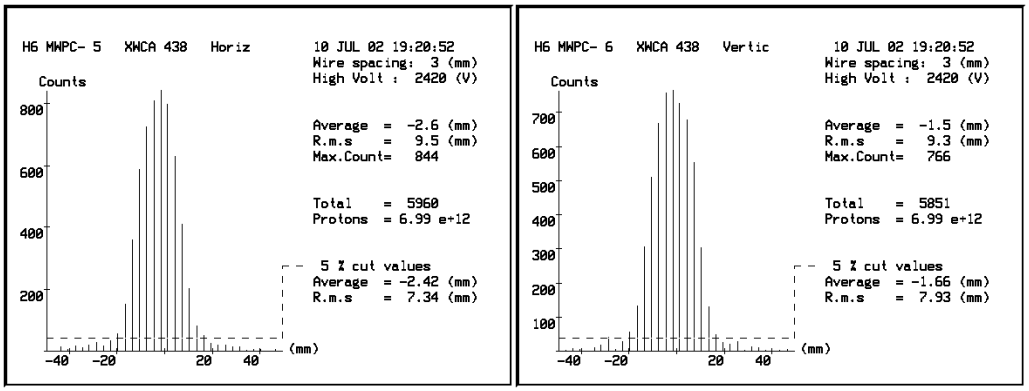

Figure 1. Horizontal and vertical beam profiles measured with the MWPC installed one metre upstream of the copper target under the concrete roof-shield. The beam intensity was $3x10^7$ particles per spill.

3. Performance tests of the BIG PIC

The Precision Ionisation Chamber (PIC) [5], the primary beam monitor at CERF, had until now no back-up instrument. Since all measurements at CERF are normalised to unit beam particle incident on the copper target, the importance of the PIC is apparent. Therefore, a second beam monitor was tested, installed in the facility and inter-compared to the PIC, in order to have it characterised and ready for use in case of a PIC failure in any future run.

This second device was built at CERN about 25 years ago, at the same time as the standard PIC. It is a 4.9-litre effective volume open-air ionisation chamber of the same design as the PIC (i.e., of cylindrical shape), with identical external cross-sectional area. Knowing the effective volume and the diameter of the chamber one can calculate its effective length, which is 99.8 mm. This is 3.1 times the effective length of the PIC, which is 32 mm [5]. For this reason this device is called here the BIG PIC. From this result we expect that the sensitivity of the BIG PIC is approximately three times the sensitivity of the PIC (as it was verified by the experimental results discussed in section 3.2). The technical characteristics of the BIG PIC are summarised in table A1 in the Appendix.

The device is connected to a high-voltage power supply and digitiser housed in a small metal box. In this box, a small electronic device manufactured by HAMAMATSU and referenced C4960-1 provides the high-voltage supply with a very good stability and linearity. The voltage can be adjusted from 0 Volts to –1250 Volts (in the following, all voltage values are meant negative polarity). Under normal conditions the chamber is operated at 600 Volts. Two S-HVS connectors are used for the power supply of the chamber and for the control of the output voltage. A digitiser, with a sensitivity of 1 pC/digit, converts the input current to an output frequency.

There are 2 connectors LEMO 00, one for connecting the chamber and the other for checking and recording the output frequency.

The BIG PIC was submitted to a number of performance tests similar to those made in the past on the PIC (see refs. [6,7] for a more detailed description of the methods adopted here). Measurements were performed in the TIS/RP calibration laboratory on 4th and 5th July, to verify the region of ion saturation, the linearity of the response versus intensity of the radiation field, the stability and the leakage current of the chamber. The BIG PIC was then tested in the hadron beam at CERF during the July run, and its response was compared to that of the standard PIC. Measurements of the instrument stability were repeated in August in the calibration laboratory after the CERF runs.

3.1 Measurements in the calibration laboratory

All measurements in the calibration laboratory were performed at the nominal voltage of 600 V, except for the determination of ion saturation for which the voltage was varied between 10 V and 1000 V. Air pressure and ambient temperature were sufficiently stable throughout the measurements that no corrections had to be applied. There were some variations in the humidity, but this parameter has only a minor influence on the operation of the chamber [8].

To investigate the warming up time of the electronics, i.e. the time needed to reach stable operating conditions, measurements were performed for seven hours after switching on the power. The first stability test was performed on the 5th July. Measurements were performed with ^{137}Cs sources of different activities providing air kerma rates varying between 10 μGy/h and 30 mGy/h. For the air kerma rates of 10 μGy/h up to 300 μGy/h the measuring time was 1000 s for each measurement. The measurements with air kerma rates between 500 μGy/h and 3 mGy/h lasted 300 s each, while measurements at the highest air kerma rates lasted 100 s each. The sources used, the values of air kerma rates and the duration of the measurements are summarised in Table A2 in the Appendix. The air pressure, temperature and humidity in the calibration laboratory were recorded before each measurement. The pressure and the temperature were fairly stable, P = (968.7 ± 1.0) hPa and T = (19.8 ± 1.0) ^{0}C, respectively. The humidity varied in the range 43.3% to 73%, which translates in a variation of 2% on the reading of the chamber [8].

This first stability test indicated that after several hours the chamber might still not have reached stable operating conditions. The stability test was therefore repeated over a longer period (72 hours) on 5th-8th August. For this series of measurements only one source was used, providing an air kerma rate of 3 mGy/h. The measuring time for the first four measurements was 1000, 900, 300 and 360 s, respectively, and 300 s for all the other measurements. The air pressure and temperature in the calibration laboratory were recorded before each measurement and were found again stable, P = (960.3 ± 1.0) hPa and T = (19.4 ± 1.0) ^{0}C, respectively. The humidity varied in the range 53.4% to 72.3%. The results of the July and August measurements are plotted together in Figure 2. The slight difference between the values of air pressure in the two periods corresponds to a variation in the sensitivity of the chamber of approximately 1%. Since this is a minor correction, it was not accounted for. The results of the August measurements alone are plotted in Figure 3. The results of the two series of measurements indicate that the BIG PIC needs almost ten hours to stabilise.

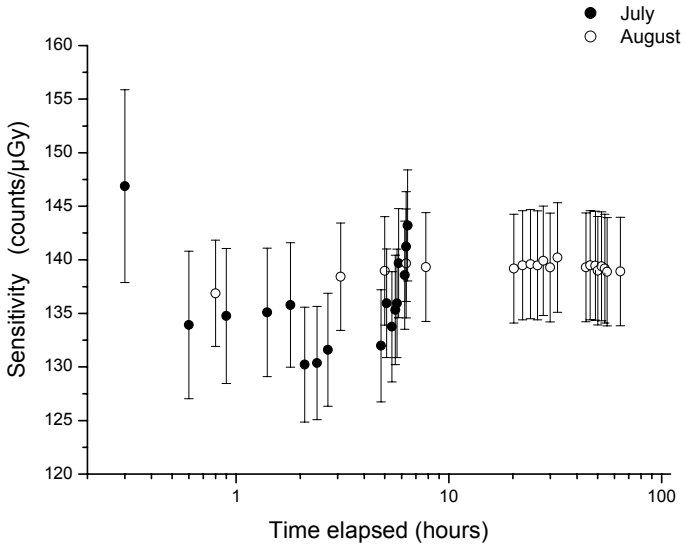

Figure 2. Stability test of the BIG PIC: sensitivity of the chamber as a function of time after switching it on. The error bars include the statistical uncertainties of the measurement, the 2% variation with humidity and the 3% uncertainty on the source output.

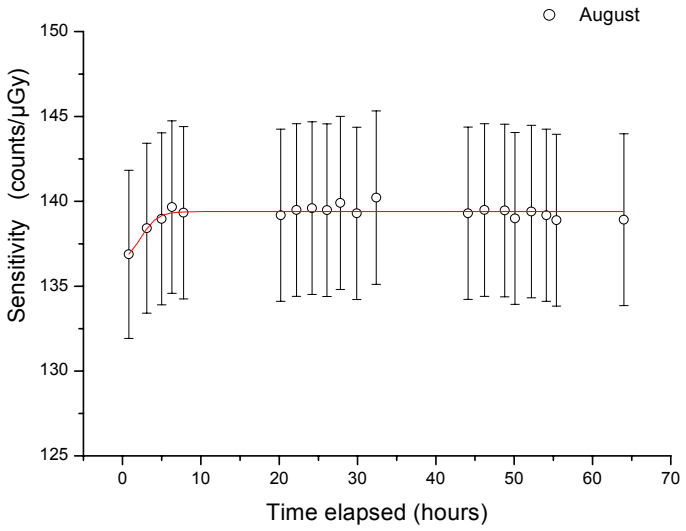

Figure 3. Stability test of the BIG PIC: sensitivity of the chamber as a function of time after switching it on. The error bars include the statistical uncertainties of the measurement, the 2% variation with humidity and the 3% uncertainty on the source output. The line is only to guide the eye.

To test the linearity of the response of the BIG PIC, the chamber was irradiated with ^{137}Cs sources providing air kerma rates in the range 10 µGy/h to 30 mGy/h. Table A2 in the Appendix lists the relevant parameters of the irradiations

(source identification, air kerma rates, number and duration of measurements). The results, shown in Figure 4, indicate a good linearity of the response in the entire interval investigated. The parameters of the linear fit are given on the plot. We just recall here that the chi-square (X^2) over the degrees of freedom N-m (where N is the number of data points and m is the number of parameters estimated by the fit) is the reduced chi-square. The values of the reduced chi-square corresponding to the probability $P_x(x^2; N\text{-}m)$ of exceeding x^2 versus the number of degrees of freedom are tabulated in textbooks [9].

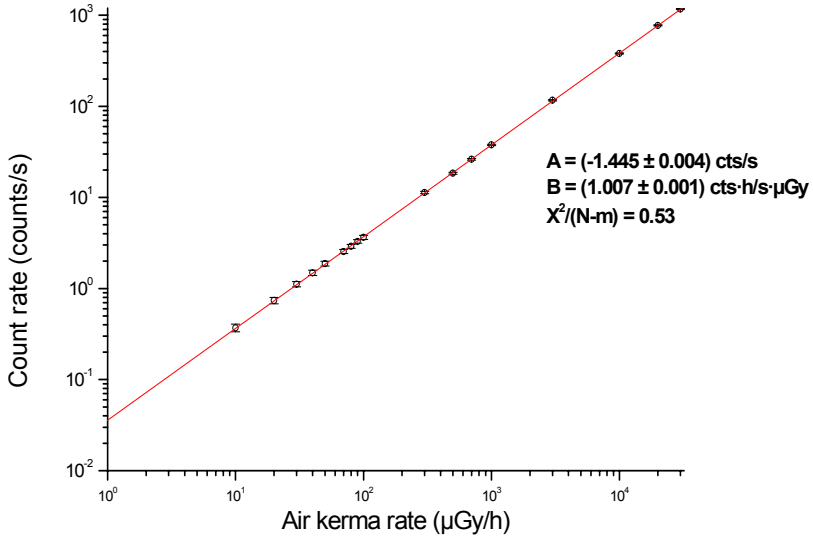

Figure 4. Linearity test of the BIG PIC: measured count-rate (counts per second) versus air kerma rate. The line is a linear fit $Y = A + B X$ to the experimental data, with $Y = \log_{10} y$ and $X = \log_{10} x$.

The region of ion saturation (i.e., the region in which there is no ion recombination in the chamber), which determines the operating region of the instrument, was evaluated with a series of measurements made with a ^{137}Cs source (source id: Cs2045). The chamber was exposed to an air kerma rate of 30 mGy/h at a distance of 1.56 m from the source. The voltage applied to the chamber was varied from 10 V to 1000 V in steps of 50 V (except for the first two measurements, where the step was 20 V). For each voltage setting three measurements were made of duration 20 to 60 s. The results are listed in Table A3 in the Appendix and are plotted in Figure 5. The figure shows that the nominal operating voltage of 600 V lies well within the region of ion saturation for photon air kerma rates of up to 30 mGy/h, which is the maximum one available in the calibration laboratory.

Another test made on the BIG PIC was the investigation of leakage current. A leakage in the capacity of the digitiser would modify the response of the chamber to a pulsed radiation field like at CERF, where the beam comes in pulses lasting a few seconds and spaced by about 13 seconds. To investigate this effect, the data from the linearity test were divided by the air kerma rate and plotted as a function of kerma rate in Figure 6. The data and the fit seem to indicate the absence of leakage current in the

interval of air kerma rate investigated, in agreement with the results of the linearity test shown in Figure 4. Only in the region of very low air kerma rates (below 10 µGy/h) no conclusions can actually be drawn. To verify the absence of a small leakage current, which would cause a deviation from linearity, additional measurements at low kerma rates (< 10 µGy/h) are needed, to simulate the behaviour of the chamber for very low intensities of the CERF hadron beam.

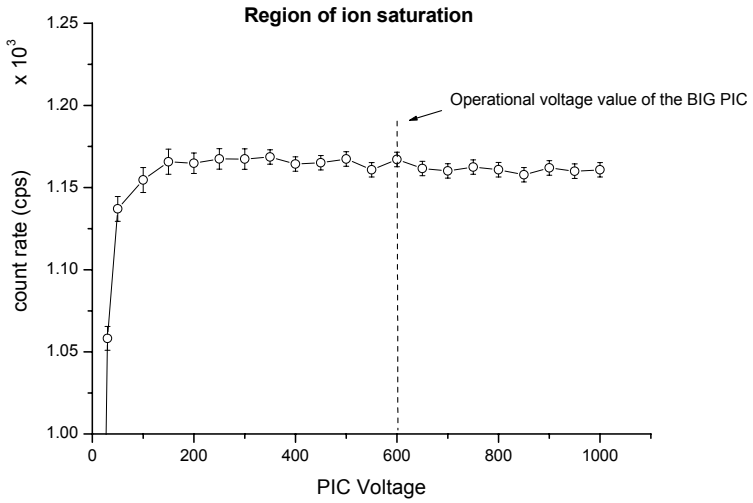

Figure 5. Count-rate versus applied voltage showing the region of ion saturation of the BIG PIC. The line is only to guide the eye.

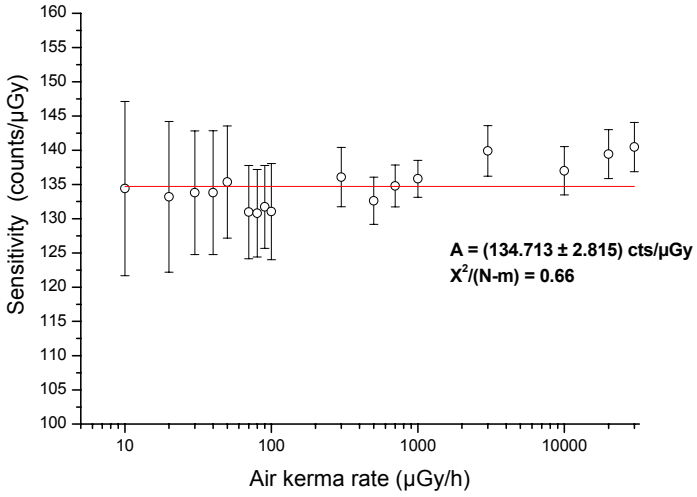

Figure 6. Sensitivity versus air kerma rate of the BIG PIC. The line is a fit y = A to the experimental data.

Long-term measurements also showed that the electronics of the chamber is not affected by any noise (i.e., the chamber did not show any spurious counting in the course of the test).

3.2 Measurements at CERF

The BIG PIC was tested at CERF during the June and July 2002 runs. The chamber was installed in the beam about one metre downstream of the standard PIC. Preliminary tests were carried out in June and measurements were performed in July, to inter-compare the response of the two beam monitors and to verify the presence of any recombination effect while operating the BIG PIC in a hadron beam.

In order to inter-compare the response of the BIG PIC to that of the PIC, the readings of the two instruments were recorded over a number of SPS pulses and for several beam intensities. The results are given in Table A4 in the Appendix and are plotted in Figure 7. Since the distance traversed by the particles in the active volume of the BIG PIC is 3.1 times the distance traversed in the standard PIC (see above), one expects that the ratio of the readings of the two instruments is about 3, plus or minus an uncertainty which is ± 5% for the PIC [10] and can reasonably be assumed of the same order for the BIG PIC. From Table A4 and Figure 7 one sees that the ratio between the readings of the BIG PIC and the PIC ranges from 3.09 at low beam intensities (200 PIC-counts per spill) down to 2.95 for very high intensities. These variations are well within the experimental uncertainties and in agreement with the above factor. Nonetheless, the ratio seems to show a slightly decreasing trend with increasing intensity of the hadron beam starting at about 6000 PIC/ spill (see below).

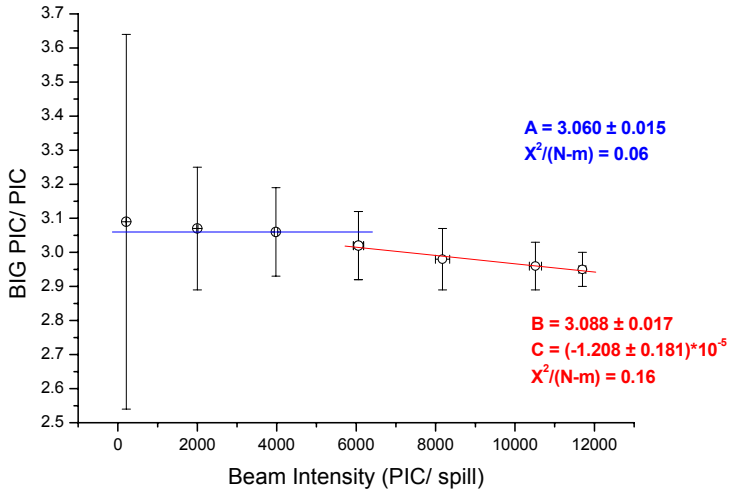

Figure7. Ratio of the reading of the BIG PIC to that of the PIC as a function of beam intensity. The lines are fits Y = A and Y = B + Cx to the experimental data.

It has previously been demonstrated that the standard PIC is not subjected to charge recombination when exposed to the CERF beam (120 GeV/c positive hadrons, about 2/3 pions and 1/3 protons) and that its response remains constant with increasing beam intensity [7]. The above results may therefore suggest a small recombination effect at high intensity in the BIG PIC. To verify this hypothesis, a

series of measurements were performed to obtain saturation curves of the chamber (i.e, voltage characteristics curves) for different beam intensities.

The beam intensity was varied by adjusting collimators 3 and 5; all others were left at their nominal CERF settings (i.e., collimators C1 and C2 set at ± 20, and C8 to C11 fully open). The beam intensity was varied between 200 and 14000 PIC-counts (of the standard PIC monitor) per spill (which corresponds to three times higher count-rates of the BIG PIC). Beam intensities and fluctuations are summarised in Table A5 in the Appendix. For each collimator setting, data were taken by varying the voltage applied to the BIG PIC from 10 V to 1000 V. The reading of the chamber was corrected for slight beam intensity fluctuations by recording the number of primary protons impinging on the T4 production target according to the expression:

$$\left\langle \frac{BIG\ PIC-counts/spill}{p_{T4}/spill}\Big|_{V} \right\rangle \cdot \left\langle p_{T4}/spill \right\rangle\Big|_{collset} \qquad (1)$$

For each voltage settings five readings of the BIG PIC per spill and the corresponding proton intensities on the T4 target were recorded. As discussed in ref. [7], expression (1) represents the average of the count-rates (BIG PIC-counts/spill) normalised to the proton rate on T4 (p_{T4}/spill) for one voltage setting, multiplied by the mean proton rate for each collimator setting.

The above quantity is plotted in Figure 8 as a function of the voltage applied to the BIG PIC, for various beam intensities. The graph seems to confirm the existence of a slight ion recombination effect in the chamber for beam intensities above about 6000 counts/spill.

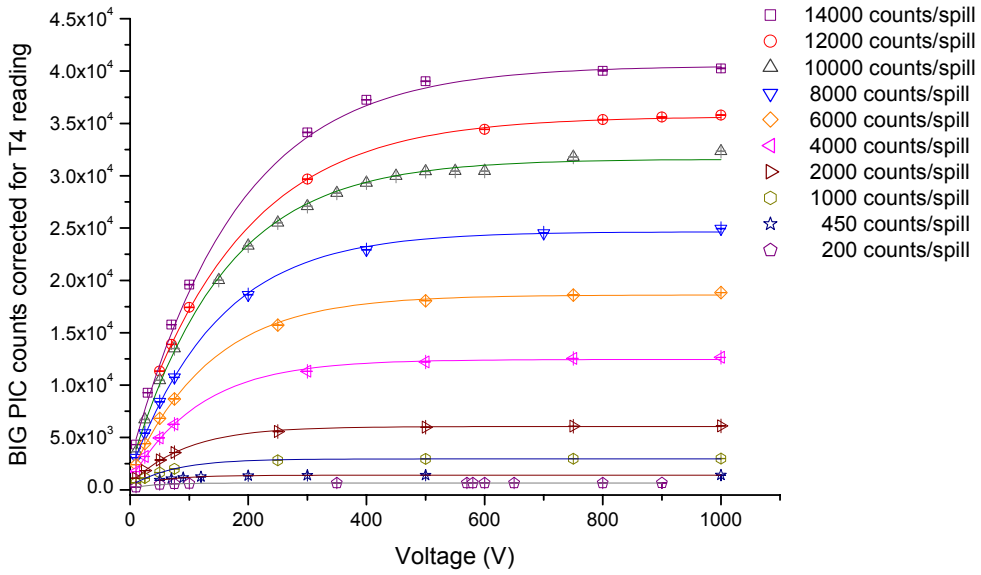

Figure 8. Voltage characteristic curves of the BIG PIC for different beam intensities at CERF. The count-rates are corrected for slight beam fluctuations. The uncertainties associated to the data points range from 0.14% to 2.13% and are too small to appear in the plot. The lines are sigmoidal fits to the data to guide the eye.

4. HANDI TEPC and rem counter measurements

Measurements of the dose equivalent at the various CERF reference exposure locations were performed with the HANDI TEPC and the rem counter LINUS. Measurements were carried out in almost all positions on the concrete top, iron top and concrete side. As usual, the measurements were performed in the centre of the 50 x 50 cm^2 reference exposure positions at approximately 25 cm above floor on the concrete top and iron top, and at the beam height on the lateral position. The results are listed in Tables 1-3. The tables give the total dose equivalent, the low LET (< 6 keV/μm) and the high LET (> 6 keV/μm) components as measured by the HANDI, the neutron ambient dose equivalent as measured by the LINUS and the FLUKA reference values for neutrons from ref. [1]. The latter were obtained by folding the neutron spectral fluence calculated by FLUKA at each reference position with the fluence-to-ambient dose equivalent conversion coefficients of ICRP74 [11] and of Ferrari and Pelliccioni [12].

The HANDI data compare well with results of previous measurements [13]. There is also overall agreement between the high-LET values of the HANDI, the results of LINUS and the FLUKA values. The only exception stands for the LINUS results on the iron roof-shield, which are systematically higher than both the HANDI and the FLUKA values. This is probably due to the fact that the LINUS (and rem counters in general) overestimates the ambient dose equivalent in the energy interval from a few keV to about 100 keV [14], a region that gives a substantial contribution to the neutron spectrum outside the iron shield [1]. To verify this assumption the FLUKA neutron spectrum was folded with the response function of the LINUS, to estimate the expected count rate of the instrument. From thermal up to 19.6 MeV both the spectrum and the response function use 72 energy groups. Above this energy the response of the LINUS is given at discrete values [14]. A polynomial fit (Figure 9) was used to interpolate the response function between 19.6 MeV and 2 GeV. Different fits produced very little variations on the final results of the folding procedure. The results (the estimated count rate multiplied by the LINUS calibration factor to yield dose equivalent rate) are compared with the experimental data in Table 4. Except for a few exposure positions where the experimental data exceed the calculated values by 25% to 30%, the quite good agreement between measurements and estimates confirms the above hypothesis.

5. Conclusions

The beam set-up at CERF is made much easier by the MWPC recently installed in the irradiation cave close to the copper target. The beam profile in the horizontal and vertical planes can now be measured on-line.

The BIG PIC seems slightly less performing than the standard CERF beam monitor (the PIC): it shows a comparatively long warm-up time and a slight recombination at high beam intensities. The BIG PIC was built about 25 years ago at the same time as the standard PIC, but unfortunately its “history” is not known. The present results seem to indicate that its characteristics and performance are sufficient as a back-up instrument to the primary CERF beam monitor, but some corrections for ion recombination might have to be applied at high beam intensity.

The mapping of the reference exposure locations with the HANDI TEPC and the LINUS rem counter has shown values in agreement with past measurements.

Acknowledgements

We wish to thank I. Efthymiopoulos and colleagues of the SL/EA and SL/BI-EA groups for setting up the MWPC. We are also indebted to D. Perrin and M. Pangallo for building the power supply of the BIG PIC and for useful advice. We also wish to thank A. Mitaroff for useful discussions and C. Raffnsøe for providing us with information on the technical characteristics of the BIG PIC.

Table 1. Dose equivalent rates on top of the concrete roof-shield (concrete top, CT). The values are in 10^{-10} Sv/PIC-count. The LINUS and FLUKA values are for neutrons and should be compared with the high-LET values of the HANDI.

Pos.	PIC/spill	HANDI TEPC			LINUS (neutrons)	FLUKA (neutrons)
		Total	High LET	Low LET		
CT1	2500	2.86 ± 0.19	2.30 ± 0.17	0.56 ± 0.03	2.07 ± 0.23	**2.16**
CT2	3400	3.20 ± 0.21	2.56 ± 0.19	0.64 ± 0.03	2.20 ± 0.33	
	4150	2.88 ± 0.18	2.36 ± 0.16	0.52 ± 0.03	2.03 ± 0.17	
	Average		**2.46 ± 0.25**		**2.12 ± 0.37**	**2.25**
CT3	3100	2.74 ± 0.17	2.23 ± 0.15	0.51 ± 0.03	2.02 ± 0.22	**2.13**
CT4	6000	2.18 ± 0.13	1.84 ± 0.11	0.34 ± 0.02	1.56 ± 0.16	**1.85**
CT5	6500	3.30 ± 0.20	2.63 ± 0.18	0.67 ± 0.03	2.56 ± 0.22	**2.54**
CT6	3000	3.89 ± 0.24	3.00 ± 0.21	0.89 ± 0.05	2.62 ± 0.22	**2.70**
CT7	2100	3.94 ± 0.24	3.09 ± 0.21	0.85 ± 0.04	2.66 ± 0.27	**2.67**
CT8	500	3.03 ± 0.20	1.48 ± 0.15	1.55 ± 0.08	—	
	1150	3.60 ± 0.23	2.34 ± 0.19	1.26 ± 0.06	2.20 ± 0.30	
	6000	2.75 ± 0.16	2.25 ± 0.14	0.50 ± 0.03	2.12 ± 0.16	
	Average		**2.02 ± 0.28**		**2.16 ± 0.34**	**2.23**
CT9	2500	4.03 ±0.26	3.03 ± 0.22	1.00 ± 0.05	2.56 ± 0.25	**2.53**
CT10	2050	4.37 ± 0.28	3.33 ± 0.24	1.04 ± 0.05	2.73 ± 0.24	
	6500	3.64 ± 0.22	2.98 ± 0.19	0.66 ± 0.03	2.81 ± 0.25	
	Average		**3.16 ± 0.31**		**2.77 ± 0.35**	**2.70**
CT11	6500	3.72 ± 0.23	3.13 ± 0.21	0.59 ± 0.03	2.73 ± 0.23	**2.65**
CT12	5000	3.13 ± 0.18	2.54 ± 0.16	0.59 ± 0.03	2.20 ± 0.17	
	5500	3.19 ± 0.19	2.62 ± 0.17	0.57 ± 0.03		
	Average		**2.58 ± 0.23**		**2.20 ± 0.17**	**2.21**
CT13	1150	3.98 ± 0.29	2.48 ± 0.24	1.50 ± 0.08	2.11 ± 0.24	
	4150	3.05 ± 0.17	2.43 ± 0.15	0.62 ± 0.03	2.15 ± 0.21	
	Average		**2.46 ± 0.28**		**2.13 ± 0.32**	**2.07**
CT14	3400	3.86 ± 0.24	2.92 ± 0.21	0.94 ± 0.05	2.33 ± 0.23	**2.22**
CT15	6500	3.13 ± 0.19	2.56 ± 0.17	0.57 ± 0.03	2.23 ± 0.22	**2.07**
CT16	5000	2.64 ± 0.15	2.16 ± 0.13	0.48 ± 0.02	1.80 ± 0.17	
	5500	—	—	—	1.82 ± 0.18	
	Average		**2.16 ± 0.13**		**1.81 ± 0.25**	**1.82**

Table 2. Dose equivalent rates on top of the iron roof-shield (iron top, IT). The values are in 10^{-10} Sv/PIC-count. The LINUS and FLUKA values are for neutrons and should be compared with the high-LET values of the HANDI.

Pos.	PIC/spill	HANDI TEPC			LINUS (neutrons)	FLUKA (neutrons)
		Total	High LET	Low LET		
IT1	1100	11.19 ± 0.80	9.96 ± 0.76	1.23 ± 0.06	13.17 ± 0.85	**10.41**
IT2	1100	12.03 ± 0.86	10.70 ± 0.81	1.33 ± 0.07	16.31 ± 0.97	**11.70**
IT3	1100	14.62 ± 1.00	12.90 ± 0.95	1.72 ± 0.09	13.74 ± 0.88	**12.38**
IT4	280	15.50 ± 1.16	11.30 ± 1.03	4.20 ± 0.21	17.42 ± 1.13	**11.37**
IT5	1450	13.64 ± 0.88	12.30 ± 0.83	1.34 ± 0.07	16.49 ± 0.91	**12.86**
IT6	1000	16.40 ± 1.09	13.90 ± 1.00	2.50 ± 0.13	21.06 ± 1.45	**14.90**
IT7	1100	18.71 ± 1.17	16.60 ± 1.09	2.11 ± 0.11	23.93 ± 1.13	**16.02**
IT8	1450	16.89 ± 1.07	15.70 ± 1.02	1.19 ± 0.06	23.41 ± 0.99	**14.93**
IT9	—	—	—	—	—	**12.03**
IT10	1000	17.39 ± 1.52	15.40 ± 1.47	1.99 ± 0.10	21.33 ± 1.13	**14.54**
IT11	—	—	—	—	—	**15.96**
IT12	1450	17.27 ± 1.02	16.30 ± 0.99	0.97 ± 0.05	24.34 ± 1.09	**14.71**
IT13	1100	10.62 ± 0.75	8.03 ± 0.66	2.59 ± 0.13	10.84 ± 0.78	**7.32**
IT14	—	—	—	—	—	**10.02**
IT15	1100	13.98 ± 0.94	11.40 ± 0.84	2.58 ± 0.13	19.00 ± 1.02	**10.99**
IT16	280	18.99 ± 1.26	12.20 ± 1.02	6.79 ± 0.34	16.90 ± 1.16	
	1450	12.83 ± 0.83	11.30 ± 0.77	1.53 ± 0.08	16.95 ± 0.91	
	Average		**11.75 ± 1.28**		**16.92 ± 1.47**	**10.05**

Table 3. Dose equivalent rates alongside the 80-cm thick concrete side-shield (concrete side, CS), i.e. with the copper target placed under the concrete roof-shield. The values are in 10^{-10} Sv/PIC-count. The LINUS values are for neutrons and should be compared with the high-LET values of the HANDI.

Pos.	PIC/spill	HANDI TEPC			LINUS (neutrons)
		Total	High LET	Low LET	
CS1	6600	5.02 ± 0.29	**4.36 ± 0.26**	0.66 ± 0.03	**3.44 ± 0.27**
CS2	6600	4.89 ± 0.28	**4.24 ± 0.26**	0.65 ± 0.03	**3.46 ± 0.26**
CS3	6600	4.61 ± 0.27	**4.03 ± 0.24**	0.58 ± 0.03	**3.38 ± 0.25**
CS4	6600	3.78 ± 0.23	**3.34 ± 0.21**	0.44 ± 0.02	**2.87 ± 0.23**
CS5	—	—	—	—	—
CS6	6600	3.64 ± 0.22	**3.18 ± 0.20**	0.46 ± 0.02	**2.69 ± 0.23**
CS7	6600	3.34 ± 0.21	**2.93 ± 0.19**	0.41 ± 0.02	**2.53 ± 0.29**
CS8	6600	2.80 ± 0.18	**2.47 ± 0.17**	0.33 ± 0.02	**2.15 ± 0.20**

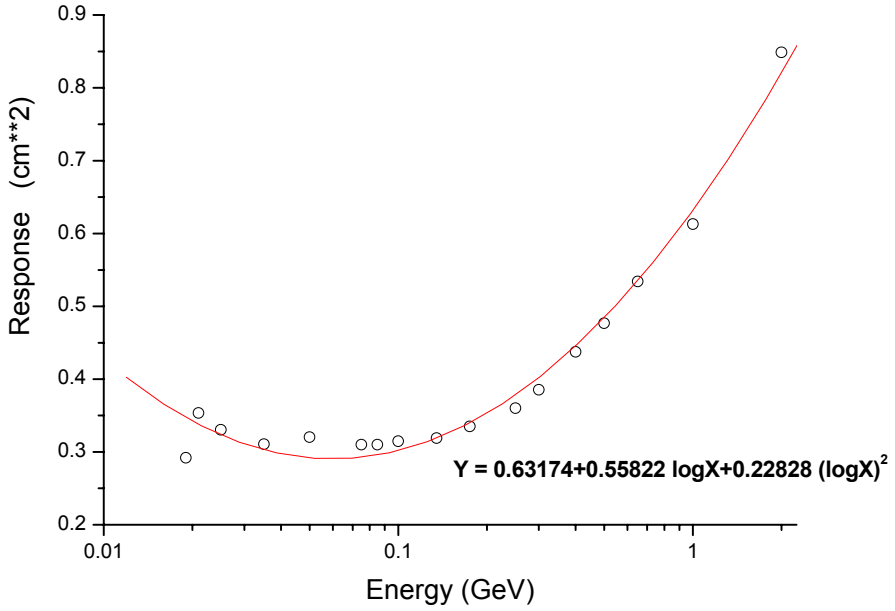

Figure 9. High-energy part (19.6 MeV to 2 GeV) of the LINUS response function with the polynomial fit used for folding it with the FLUKA spectrum on the iron roof-shield of CERF.

Table 4. Dose equivalent rates on top of the iron roof-shield (iron top, IT): comparison between experimental data and values calculated by folding the FLUKA neutron spectrum with the LINUS response function. The last column gives the FLUKA reference values for neutrons (from ref. [1]) as in Table 2. The values are in 10^{-10} Sv/PIC-count.

IT Position	LINUS (calculated)	LINUS (experimental)	LINUS (exp-calc) / LINUS (exp) (%)	FLUKA
1	12.70	13.17	3.57	10.41
2	14.30	16.31	12.32	11.70
3	15.11	13.74	-9.97	12.38
4	13.92	17.42	20.10	11.37
5	15.66	16.49	5.03	12.86
6	18.32	21.06	13.01	14.90
7	19.53	23.93	18.39	16.02
8	19.11	23.41	18.37	14.93
10	17.73	21.33	16.88	14.54
12	18.11	24.34	25.60	14.71
13	8.87	10.84	18.17	7.32
15	13.33	19.00	29.84	10.99
16	12.36	16.90	26.86	10.05

References

1. A. Mitaroff and M. Silari, *The CERN-EU high-energy Reference Field (CERF) facility for dosimetry at commercial flight altitudes and in space*, Radiation Protection Dosimetry 102, 7-22 (2002). See also http://www.cern.ch/cerf.
2. E. Efthymiopoulos, A. Mitaroff and M. Silari, *Efficiency measurements of the Trigger4 beam monitor in H6*, Technical Note CERN/TIS-RP/TN/2002-027 (2002).
3. T. Otto and M. Silari, *The July/August 1996 run at the CERN-CEC reference facility*, Technical Memorandum CERN/TIS-RP/TM/96-25 (1996).
4. T. Otto and M. Silari, *The May 1996 run at the CERN-CEC reference field facility*, Internal Report CERN/TIS-RP/IR/96-15 (1996).
5. R.C. Raffnsøe, *Instrumentation for beam experiments in North Hall*, Technical Memorandum TIS-RP-DC/TM/92-27 (1992).
6. E. Gschwendtner, A. Mitaroff and T. Otto, *Performance tests of the CERF beam monitor*, Technical Memorandum CERN/TIS-RP/TM/2000-07 (2000).
7. A. Mitaroff and T. Otto, *Recombination measurements of the CERF beam monitor for a 120 GeV/c hadron beam*, Internal Report CERN/TIS-RP/IR/2002-028 (2002).
8. R. G. Jaeger and W. Hübner , Dosimetrie und Strahlenschutz, 1974 (in German).
9. P.R. Bevington and D. Keith Robinson, *Data Reduction and Error Analysis for the Physical Sciences*, McGraw-Hill, 2nd Edition, (1992).
10. E. Gschwendtner, A. Mitaroff and L. Ulrici, *A new calibration of the PIC monitor in H6*, Internal Report CERN/TIS-RP/IR/2000-09 (2000).
11. International Commission on Radiological Protection, *Conversion coefficients for use in radiological protection against external radiation,* Publication 74 (Oxford: Pergamon Press) (1996).
12. A. Ferrari and M. Pelliccioni, *Fluence to dose equivalent conversion data and effective quality factors for high energy neutrons*, Radiat. Prot. Dosim. 76, 215-224 (1998).
13. E. Dimovasili, S. Mayer, A. Mitaroff and M. Silari, *HANDI TEPC measurements during the 1999, 2000 and 2001 CERF runs*, Technical Note CERN/TIS-RP/TN/2000-020 (2002).
14. C. Birattari, A. Esposito, A. Ferrari, M. Pelliccioni, T. Rancati and M. Silari, *The extended range neutron rem counter 'LINUS': overview and latest developments*, Radiat. Prot. Dosim. 76, 135-148 (1998).

APPENDIX

Table A1. Technical characteristics of the BIG PIC.

Parallel Plate Chamber for monitoring high energetic beams of moderate intensity	
Plate spacing	50 mm
Effective Diameter	250 mm
Aperture	185 mm
Effective volume	4.9 litres
Surface area	490 cm^2
Electrodes	Aluminized mylar foil
Electrode thickness	2.5 mg/cm^2
Total Chamber thickness	35.5 mg/cm^2

Table A2. ^{137}C source identification, air kerma rate, duration and number of measurements performed for the July stabilisation test and the linearity test of the BIG PIC performed in the TIS/RP calibration laboratory.

Source	Air kerma rate (µGy/h)	Stabilisation test	Linearity test	
		Duration (s)	Duration (s)	Repetition
Cs3739	10	1000	10	30
	20	1000	10	20
	30	1000	10	20
	40	1000	10	15
	50	1000	10	15
Cs3740	70	1000	10	15
	80	1000	10	15
	90	1000	10	15
	100	1000	10	10
	300	1000	10	10
Cs3609	500	300	10	10
	700	300	10	10
	1000	300	10	10
	3000	300	100	2
Cs2045	10000	100	100	2
	20000	100	100	2
	30000	100	100	2

Table A3. Average count rate versus applied voltage for the determination of the region of ion saturation of the BIG PIC.

Voltage (V)	Average count rate (counts per s)	Voltage (V)	Average count rate (counts per s)
10	623.47 ± 5.58	500	1167.43 ± 4.41
30	1058.23 ± 7.27	550	1160.83 ± 4.40
50	1137.08 ± 7.54	600	1167.14 ± 4.41
100	1154.63 ± 7.60	650	1161.59 ± 4.40
150	1165.75 ± 7.63	700	1160.16 ± 4.40
200	1164.86 ± 6.23	750	1162.48 ± 4.40
250	1167.46 ± 6.24	800	1160.88 ± 4.40
300	1167.40 ± 6.24	850	1157.83 ± 4.39
350	1168.63 ± 4.41	900	1161.94 ± 4.40
400	1164.32 ± 4.41	950	1159.96 ± 4.40
450	1165.14 ± 4.41	1000	1160.80 ± 4.40

Table A4. Inter-comparison of the two CERF beam monitors (the standard PIC and the BIG PIC) in the hadron beam at CERF. The total PIC and BIG PIC values are the sum of the readings of the single pulses. The uncertainty associated to the ratio in the last column has been computed by the usual error propagation formula.

Beam intensity (PIC/spill)	Average beam intensity (PIC/spill)	BIG PIC	Total PIC	Total BIG PIC	BIG PIC/PIC
11598	11696 ± 86	34259	35089	103681	2.95 ± 0.05
11759		34761			
11732		34661			
10507	10514 ± 151	31154	52570	155700	2.96 ± 0.07
10648		31553			
10293		30510			
10461		31038			
10661		31445			
7978	8175 ± 181	23754	40873	121669	2.98 ± 0.09
7991		23802			
8229		24504			
8371		24887			
8304		24722			
6057	6058 ± 129	18217	30292	91441	3.02 ± 0.10
6238		18743			
6105		18372			
5889		17721			
6003		18388			
3951	3981 ± 41	12060	19905	60892	3.06 ± 0.13
3994		12220			
4025		12314			
3927		12023			
4008		12275			
1991	2002 ± 16	6116	10008	30733	3.07 ± 0.18
2000		6142			
2002		6140			
2028		6234			
1987		6101			
212	212 ± 1	656	1060	3273	3.09 ± 0.55
212		654			
213		657			
212		655			
211		651			

Table A5. Parameters during the measurements of the voltage characteristic curves of the BIG PIC in the hadron beam at CERF.

Nominal beam intensity (PIC/spill)	Actual beam intensity (PIC/spill)	Beam fluctuation (%)	Collimator settings	
			C3	C5
14000	13650	2.14	± 22	± 22
12000	11650	1.91	± 19	± 19
10500	10600	2.00	± 17	± 17
8000	8250	1.36	± 14	± 15
6000	6100	0.86	± 12	± 12
4000	4000	0.54	± 9	± 10
2000	1960	0.21	± 7	± 6
1000	950	0.47	± 5	± 4
450	455	0.04	± 3	± 3
200	210	0.03	± 2	± 2